Fair Adaptive Data Rate Allocation and Power Control in LoRaWAN

Khaled Q. Abdelfadeel, Victor Cionca, Dirk Pesch
Nimbus Centre, Cork Institute of Technology, Ireland
khaled.abdelfadeel@mycit.ie, victor.cionca@cit.ie, dirk.pesch@cit.ie

Abstract—In this paper, we present results of a study of the data rate fairness among nodes within a LoRaWAN cell. Since LoRa/LoRaWAN supports various data rates, we firstly derive the fairest ratios of deploying each data rate within a cell for a fair collision probability. LoRa/LoRaWAN, like other frequency modulation based radio interfaces, exhibits the *capture effect* in which only the stronger signal of colliding signals will be extracted. This leads to unfairness, where far nodes or nodes experiencing higher attenuation are less likely to see their packets received correctly. Therefore, we secondly develop a transmission power control algorithm to balance the received signal powers from all nodes regardless of their distances from the gateway for a fair data extraction. Simulations show that our approach achieves higher fairness in data rate than the state-of-art in almost all network configurations.

I. Introduction

LoRa/LoRaWAN is considered one of the Low Power Wide Area Networks [1] that promise to connect massive numbers of low-cost wireless devices/nodes[1], thousands per cell, in a simple star topology. Nodes operate with low energy consumption and data can be transmitted over long distances, e.g. many kilometers. The wide coverage area of LoRaWAN[2] is due to its unique modulation, Long Range (*LoRa*) modulation (subsection II-A), which has a large link budget. LoRa provides multiple transmission parameters: Spreading Factor SF, Bandwidth BW, Coding Rate CR and Transmission Power TP that can be tuned to trade data rate for range, power consumption, or sensitivity.

Spreading codes associated with SFs in LoRa are pseudo-orthogonal, thus LoRa can support simultaneous transmissions using different SFs as long as none is received with significantly higher power than the others [2] [3], as otherwise the strongest signal suppresses weaker signals. Also, when multiple simultaneously transmitted signals have the same SF, the strongest signal will suppress the weaker signals if the power difference is sufficiently high [4]. This is known as the capture effect.

In our earlier work in [5] we showed that the capture effect and especially the imperfect-orthogonality of SFs can make LoRaWAN an unfair system because of the near-far problem. Transmissions from nodes that are far from the gateway are not received when colliding with transmissions from nodes closer

---

[1]We use device and node interchangeably.

[2]From here on we use LoRaWAN to refer to the whole stack and network architecture that uses LoRa modulation as defined by the LoRa Alliance.

to the gateway that have significantly higher received power. This effect is magnified by LoRaWAN's large link budget leading to large power difference between transmissions from far and near nodes. Therefore, controlling the received signal power of all nodes is important to achieve fairness.

Another source of unfairness is the data rate assigned to a node. Each data rate, defined through the combination of SF, BW and CR, experiences different airtime, thus different collision probability. The collision probability is higher when using slow data rate combinations and low when using fast combinations. Following these considerations, we propose a data rate allocation and TP control algorithm, called FADR, to achieve a fair data rate for all nodes within a LoRaWAN cell while at the same time being energy efficient.

The contributions of this paper are as follows: we firstly formulate the general fairest data rate distribution to achieve a fair collision probability among all deployed data rates in a LoRaWAN cell. Then based on this distribution, we propose FADR, a data rate allocation and TP control algorithm, to achieve a fair data rate independent of distance from the gateway while avoiding excessively high TPs in order to reduce energy consumption. We provide detailed results, comparisons and discussions to show and explain how FADR performs under various network configurations. Overall, simulations show that FADR outperforms the state-of-art in almost all network configurations.

The remainder of this paper is organized as follows: Section II provides an overview of LoRa/LoRaWAN and highlights related work. Section III describes FADR in detail. We present a detailed evaluation and discussion of FADR and comparison to the state-of-the-art in Section IV. Finally, Section V presents the conclusions.

II. Literature Review

Here we provide an overview of the LoRaWAN protocol stack and highlight related work in the LoRaWAN domain.

A. Long Range (LoRa)

LoRa is a proprietary low-cost implementation of Chirp Spread Spectrum (CSS) modulation by Semtech that provides long range wireless communication with low power characteristics [6] and represents the physical layer of the LoRaWAN stack. CSS uses wideband linear frequency modulated pulses, called *chirps* to encode symbols. A LoRa symbol covers the entire bandwidth, making the modulation robust to channel

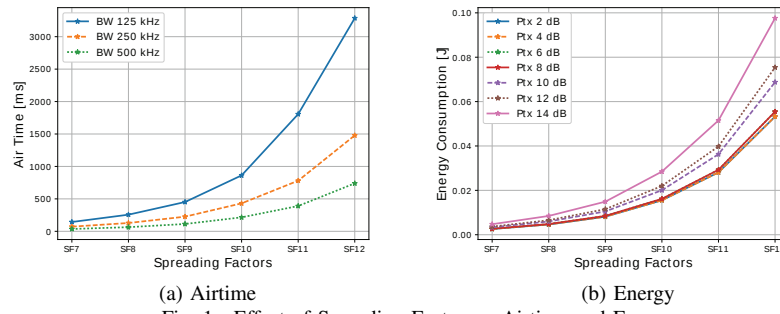(a) Airtime   (b) Energy

Fig. 1. Effect of Spreading Factor on Airtime and Energy

noise and insensitive to frequency shifts. LoRa modulation is defined by two main parameters: Spreading Factor $sf \in SFs(7,...,12)$, which affects the number of bits encoded per symbol, and Bandwidth $bw \in BWs(125, 250, 500)KHz$, which is the spectrum occupied by a symbol. A LoRa symbol consists of 2^{sf} chirps in which chirp rate equals bandwidth. LoRa supports forward error correction code rates cr equal to $4/(4+n)$ where n ranges from 1 to 4 to increase resilience. The theoretical bit rate R_b of LoRa is shown in Eq. 1 [6].

$$R_b = sf * \frac{bw}{2^{sf}} * cr \qquad bits/s \qquad (1)$$

Moreover, a LoRa transceiver allows adjusting the Transmission Power TP. Due to hardware limitations the adjustment range is limited from $2dBm$ to $14dBm$ in $1dB$ steps.

A LoRa packet can be transmitted using a constant combination of SF, BW, CR and TP, resulting in over 936 possible combinations. Tuning these parameters has a direct effect on the bit rate and hence the airtime, affecting reliability and energy consumption. Each increase in SF nearly halves the bit rate and doubles the airtime and energy consumption but enhances the link reliability as it slows the transmission. Whereas each increase in the BW doubles the bit rate and halves the airtime and energy consumption but reduces the link reliability as it adds more noise.

The airtime of a LoRa packet can be precisely calculated by the LoRa airtime calculator [7]. Fig. 1a shows the effect of SFs and BWs at code rate $CR = 4/5$ on the airtime to transmit an 80 bytes packet length. As shown, the fastest combination uses the lowest SF with the highest BW, whereas, the highest SF with the lowest BW achieves the slowest combination. Fig. 1b shows the energy consumption for combinations of SFs and TPs at $CR = 4/5$ and $BW = 500KHz$ to transmit an 80 bytes packet. As shown, the SF has much higher impact than the TP on the energy consumption, e.g. increasing SF consumes more energy than increasing TP especially for large SFs.

LoRa modulation can enable concurrent transmissions, exploiting the pseudo-orthogonality of SFs as long as none of the simultaneous transmissions is received with significantly higher power than the others [3]. Otherwise, the strongest transmission suppresses weaker transmissions if the power difference is higher than the Co-channel Interference Rejection (CIR) of weaker SFs. In case of the same SF, all simultaneous transmissions are lost, unless one of the transmissions

TABLE I
LoRaWAN Data Rates in Europe [10]

Data Rates	Parameter Combination	Indicative physical bit rate [bit/s]
0	SF12 / 125 kHz	250
1	SF11 / 125 kHz	440
2	SF10 / 125 kHz	980
3	SF9 / 125 kHz	1760
4	SF8 / 125 kHz	3125
5	SF7 / 125 kHz	5470
6	SF7 / 250 kHz	11000

is received with higher power than the CIR of the SF. This suppression of weaker signals by the strongest signal is called *capture effect* [4]. The CIR of all SF pairs has been calculated using simulations in [3] and validated by real LoRa link measurements in [8].

B. LoRaWAN

LoRaWAN [9] is an open-source Medium Access Control (MAC) layer, system architecture and regional specifications using the LoRa modulation. LoRaWAN MAC is based on simple Aloha, where a LoRa radio can transmit at any time as long as it respects the spectrum regulation. LoRaWAN operates in the Industrial Scientific and Medical (ISM) frequency band (868 MHz in Europe), which imposes a duty cycle of not more than 1% on radios that do not adopt Listen-Before-Talk (LBT). The LoRaWAN system architecture is a simple star-of-stars topology where nodes communicate directly to one or more gateways which connect to a common network server. A LoRaWAN gateway is usually equipped with multiple LoRa transceivers, thus is able to receive multiple transmissions on all transmission parameter combinations at the same time. Therefore, a LoRa device can transmit data to a network server with any transmission parameter combination without any prior configuration.

LoRaWAN defines an Adaptive Data Rate (ADR) scheme to control the uplink transmission parameters of LoRa devices. A LoRa device expresses an interest in using the ADR scheme by setting the *ADR* flag in any uplink MAC header. When the ADR scheme is enabled, the network server can control transmission parameters of a LoRa device using *LinkADRReq* MAC commands. Typically, the network server collects the 20 most recent transmissions from a node, including Signal-to-Noise Ratio (SNR) and the number of gateways that received each transmission. Based on that history, the network server

assigns transmission parameters to be more airtime and energy efficient. To reduce the *LinkADRReq* command length, not all transmission parameters are available, but a subset of only 7 (SF and BW) combinations as shown in table I and 5 TPs (2,5,8,11, or 14) can be set [9].

C. Related Work

Recent research on LoRa/LoRaWAN has mainly focused on LoRa performance evaluation in terms of coverage, capacity, scalability and lifetime. The studies have been carried out using real deployments in [11] and [12], mathematical models in [13] and [14], or computer simulations in [4] and [15]. Almost all these works have assumed perfectly orthogonal SFs although it has been shown in [2] and [8] that this is not a valid assumption.

Furthermore, recent work has proposed transmission parameter allocation approaches for LoRaWAN with different objectives. For example, authors in [16] proposed a transmission parameter selection approach for LoRa to achieve low energy consumption at a specific link reliability. Here a LoRa node probes a link using a transmission parameter combination to determine the link reliability. It then chooses the next probe combination based on whether the new combination achieves lower energy consumption while maintaining at least the same link reliability. Finally, the approach terminates when reaching the optimal combination from an energy consumption perspective.

Authors in [17] proposed two SF allocation approaches, namely EXP-SF and EXP-AT, to help LoRaWAN achieve a high overall data rate. EXP-SF equally allocates SFs to N nodes based on the Received Signal Strength Indicator (RSSI), where the first $N/6$ nodes with the highest RSSI get $SF7$ assigned and then the next $N/6$ nodes $SF8$ and so on. EXP-AT is more dynamic than EXP-SF, where the SF allocation theoretically equalizes the airtime of nodes. The two aforementioned works [16] and [17] assumed perfectly orthogonal SFs, which leads to a higher overall data rate than in reality.

In the context of our work presented here, allocating data rates and TPs to achieve data rate fairness in LoRaWAN is not well investigated, with the exception of [18], where authors proposed a power and spreading factor control approach to achieve fairness within a LoRaWAN cell. We provide an overview of [18] and a detailed comparison with our proposal in Section IV. While in general data rate and power control approaches have been well studied for cellular systems and WiFi [19] [20], we argue that these solutions are not suitable for constrained systems like LoRaWAN. The reason is that cellular based approaches require fast feedback and high data rates to work, which are not available in LoRaWAN.

In the end, an interesting work was done to ensure an interoperability between LoRaWAN and the native IoT stack i.e. IPv6/UDP/CoAP at the device level. The interoperability was done by adopting legacy solution like 6LoWPAN over LoRaWAN [21] or by developing a new header compression technique to be more suitable for the constraints of LoRaWAN [22].

III. FADR ALGORITHM

In the following we present our fair data rate allocation and power control proposal, which we call FADR, to achieve data rate fairness among nodes in a LoRaWAN cell. Firstly, we derive the fair data rate distribution in subsection III-A, which tries to achieve an equal collision probability for all deployed data rates, then we provide our TP control algorithm proposal in subsection III-B, aimed at mitigating the capture and SFs non-orthogonality effects.

A. FADR - Data Rate Allocation

Each transmission parameter combination (SF, BW, with CR) leads to a different data rate and thus airtime, which causes different collision probabilities, resulting in unfairness among nodes within a cell. Finding the fair data rate deployment ratios within a cell is therefore crucial.

SF fair distribution ratios were derived in [18] as follows:

$$p_{sf} = \frac{sf}{2^{sf}} / \sum_{i=7}^{12} \frac{i}{2^i} \qquad \forall sf \in SFs, \qquad (2)$$

where p_{sf} indicates the fraction of nodes using a specific SF. Eq. 2 has been derived by equalizing the collision probability of each SF with taking into account the constraint that the sum of all probabilities must be unity $\sum_{s=7}^{12} p_{sf} = 1$.

However, Eq. 2 does not consider the impact of BW and CR on the collision probability. Assuming all SFs will be deployed with the same BW and CR may not always be the case as the network operator may consider assigning different BW and CR to the same SF in order to achieve a different data rate, reliability, or sensitivity. Therefore, we extend Eq. 2 into Eq. 3 to consider the impact of BW in addition to SF as follows:

$$p_{sf,bw} = \frac{p_{sf} * bw}{\sum_{i \in BWs} i} \qquad \forall sf \in SFs \ \& \ bw \in BWs, \quad (3)$$

where $p_{sf,bw}$ indicates the fraction of nodes using a specific SF and BW combination. Eq. 3 is derived with respect to the constraint $\sum_{i \in BWs} p_{sf,bw} = p_{sf}$. In order to also consider the impact of CR, Eq. 3 is finally extended to Eq. 4 as follows:

$$p_{sf,bw,cr} = \frac{p_{sf,bw} * cr}{\sum_{i \in CRs} i} \forall sf \in SFs \& bw \in BWs \& cr \in CRs, \tag{4}$$

where $p_{sf,bw,cr}$ indicates the fraction of nodes using a specific SF, BW and CR combination. Eq. 4 is also derived with respect to the constraint $\sum_{i \in CRs} p_{sf,bw,cr} = p_{sf,bw}$.

Eq. 4 is the generalized form of Eq. 2, where in case of deploying all SFs with the same BW and CR, the values expressed by Eq. 4 equal the values derived with Eq. 2. Hence, the fair ratios of using a potential LoRaWAN data rate as per table I without considering CR are: $p_{12,125,cr} = 0.024$, $p_{11,125,cr} = 0.044$, $p_{10,125,cr} = 0.08$, $p_{9,125,cr} = 0.144$, $p_{8,125,cr} = 0.257$, $p_{7,125,cr} = 0.15$, and $p_{7,250,cr} = 0.3$.
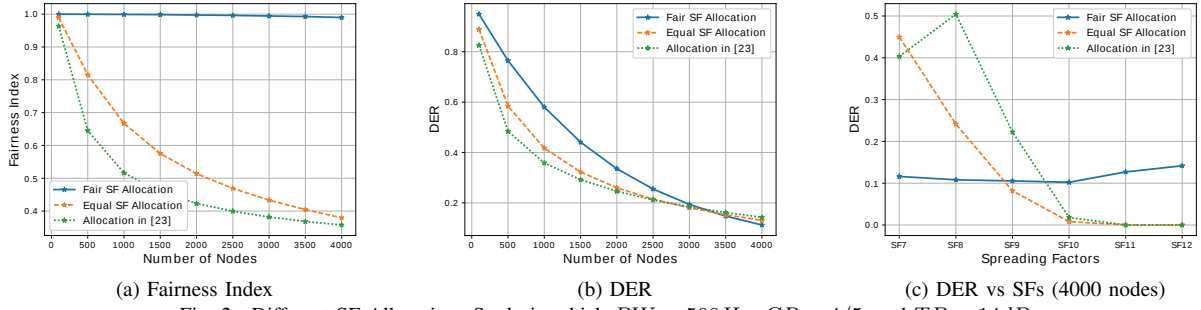
Fig. 2. Different SF Allocations Study in which $BW = 500Hz$, $CR = 4/5$, and $TP = 14dBm$

Observing Eq. 4 in allocating the data rates within Lo-RaWAN cell ensures each node has the same probability of collision. However, this leaves the question as to what is the criteria of allocating data rates over RSSI within a cell? As BWs and CRs don't affect the orthogonality, while the same is not true for SFs, which depend on the received power. We propose the region concept as a way of allocating SFs within a LoRaWAN cell. For this a LoRaWAN cell is divided into regions, where each region consists of a number of nodes that are assigned to that region based on their RSSI. Nodes per region should be allocated using the fair SF ratios from Eq. 4. We recommend that the smallest size of a region should be equivalent to representing the smallest fair ratio, which for $SF12$ equals 2% for a better representation of all ratios with in a region. Thus, we recommend the smallest region size contains 50 nodes, which means $SF12$ is used by only one node in a region. We investigate the impact of region size in section IV.

To verify the impact of the fair data rate distribution, we compared the fair data rates, assuming all nodes are within a single region, versus equal SF allocation across nodes, which has been considered in [8] and EXPLoRa-SF approach in [17], versus the proposed allocation in [23], where authors showed 28% of nodes should use $SF12$. The fairness is calculated using Jain's fairness index [24]:

$$\zeta = \frac{(\sum_{i=1}^{N} DER_i)^2}{N \sum_{i=1}^{N} DER_i^2},\tag{5}$$

where DER_i denotes the Data Extraction Rate (DER) of a node i in a cell with N nodes. The DER metric was introduced in [4] as the ratio of received packets to transmitted packets over a period of time. The fairness index varies from zero to one, where a higher index indicates a higher fairness. The results are shown in Fig. 2 for different numbers of nodes, assuming perfectly orthogonal SFs and neglecting the capture effect. This provides an insight into the fairness within a cell regardless of the assigned TPs.

Fig. 2a shows the fairness index, where the fair allocation is almost one regardless of the number of nodes. However, it dramatically degrades in the other allocations with increasing number of nodes due to increasing collisions. The impact of allocation is clear in Fig. 2c, which shows DER versus SFs for a cell of 4000 nodes. The DER for nodes using a low SF is higher than for those using a high SF with equal SF

allocation and with SF allocation as per [23]. DER is almost zero for $SF10$, $SF11$ and $SF12$, which represent half of the nodes for the equal SF allocation. This means, half of nodes cannot deliver any packets due to collisions, whereas the DER for the fair allocation is nearly equal for all SFs and around the random access limit (see Fig. 2b). The overall DER at the fair allocation outperforms the other two allocations up to about 3250 nodes. After that the overall number of collisions becomes higher, which means a lower DER than the other two allocations for the sake of equalizing the DER per SF as shown in Fig. 2c.

B. FADR - Transmission Power Allocation

The other aspect that creates unfairness in LoRaWAN is the near-far problem, which influences the capture effect, especially with not perfectly orthogonal SFs. These characteristics favor near nodes because of their higher received power than far nodes. Therefore, balancing the received powers of all nodes is required in order to achieve a fair data rate among all nodes regardless of their distance from the gateway.

Our proposed TP control algorithm is shown in Algorithm 1. The algorithm requires a list of nodes (N) with a list of corresponding RSSIs, a list of available TP levels (PowLevels) that can be assigned, and a matrix of CIR of all SF pairs as inputs (line 1). To avoid RSSI instability, the algorithm is run after a certain number of packets have been collected by the network server in order to calculate the average RSSI. RSSI stability has been investigated in [25], which showed that the RSSI standard deviation of nodes close to the gateway is less than $3dBm$, however, the deviation increases to $20dBm$ for far nodes. Algorithm 1 does not make assumptions on the initial TP assignment of the collected packets, but recommends that nodes are initiated with the same TP before running the algorithm to have RSSIs with a common reference.

Algorithm 1 allocates a TP to each node as output (line 2). The algorithm starts with sorting the nodes by their RSSI (line 3), next, calculates the maximum (MaxRSSI) and the minimum (MinRSSI) values of the measured RSSIs in addition to the minimum value of CIR (MinCIR), which represents the safe margin of all SFs (line 5). Subsequently, the algorithm finds the maximum TP (MaxPower) that can reduce the difference between RSSI extremes to below the safe margin (lines 6-13), where the minimum TP (MinPower) is the

Algorithm 1 FADR - TP Control Algorithm

1: **Input** List of nodes **N**, corresponding **RSSI**, power levels **PowLevels**, matrix of **CIR**
2: **Output** $\forall n \in \mathbf{N}, \mathbf{P}[n] \in \mathbf{PowLevels}$
3: Sort **N** by **RSSI**
4: # Calculate MinRSSI, MaxRSSI, MinCIR
5: $MinRSSI = min(\mathbf{RSSI}), MaxRSSI = max(\mathbf{RSSI}), MinCIR = min(\mathbf{CIR})$
6: **PowLevels**$.pop(0)$
7: **for all** $i \in \mathbf{PowLevels}$ **do**
8:    $MaxPower = i$
9:    **if** $|MaxRSSI + MinPower - MinRSSI - MaxPower| <= MinCIR$ **then**
10:       **PowLevels** = **PowLevels**$[0 : \mathbf{PowLevels}.index(i)]$
11:       $break$
12:    **else if** $i == max(\mathbf{PowLevels})$ **then**
13:       $powLevels.pop()$
14: # Recalculate the minimum and the maximum of **RSSI**
15: $MinRSSI = min[MinRSSI + MaxPower, MaxRSSI + MinPower]$
16: $MaxRSSI = max[MinRSSI + MaxPower, MaxRSSI + MinPower]$
17: # Assign the minimum power and save the MinPowIndex
18: **for all** $i \in range(0, len(\mathbf{N}), 1)$ **do**
19:    **if** $|\mathbf{RSSI}[i] + MinPower| > |MinRSSI|$ **then**
20:       $MinPowIndex = i - 1$
21:       $break$
22:    **else**
23:       $\mathbf{P}[i] = MinPower$
24: # Assign the maximum power and save the MaxPowIndex
25: **for all** $i \in range(len(\mathbf{N}) - 1, MinPowIndex, 1)$ **do**
26:    **if** $|\mathbf{RSSI}[i] + MaxPower - MinRSSI| > MinCIR$ **then**
27:       $MaxPowIndex = i - 1$
28:       $break$
29:    **else**
30:       $\mathbf{P}[i] = MaxPower$
31: # Assign the nodes in between with the remaining power levels
32: $TempIndex = MinPowIndex$
33: **for all** $i \in \mathbf{PowLevels}$ **do**
34:    **if** $(|\mathbf{RSSI}[TempIndex] + i - MinRSSI| <= MinCIR)$ **and** $(|\mathbf{RSSI}[TempIndex] + i - \mathbf{RSSI}[MaxPowIndex] - MaxPower| <= MinCIR)$ **then**
35:       **for all** $j \in range(TempIndex, MaxPowIndex, 1)$ **do**
36:          **if** $|\mathbf{RSSI}[j] + i - \mathbf{RSSI}[MaxPowIndex] - MaxPower| > MinCIR$ **then**
37:             $TempIndex = j - 1$
38:             $break$
39:          **else**
40:             $\mathbf{P}[j] = i$

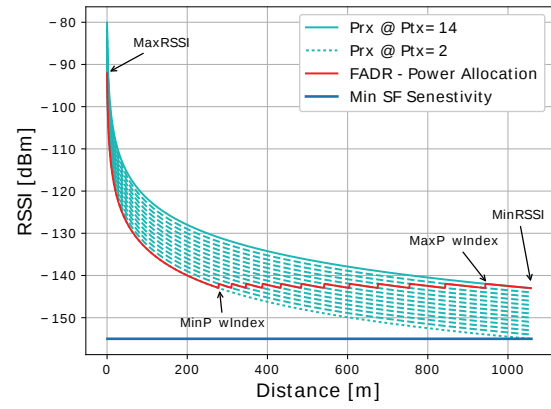
Fig. 3. FADR Power Allocation

Secondly, allocating MaxPower to low RSSI nodes as long as the new RSSI plus the safe margin is not higher than MinRSSI (line 25-30). The index of the last node that complies with this approach is saved in MaxPowIndex. Finally, the algorithm assigns to the nodes between MinPowIndex and MaxPowIndex the remaining TPs from low to high as long as the allocation of each TP complies with the rules that the new RSSI plus the safe margin is not lower than the first node using the same TP (lines 33-40).

Fig. 3 provides a visual example of how Algorithm 1 works. In Fig. 3, MinPower is $2dBm$ and MaxPower is $14dBm$ (the maximum TP for LoRaWAN) since the difference between RSSIs ($\sim 50dBm$ in that example) is higher than the difference between TPs ($12dBm$). Algorithm 1 iterates forwardly to allocate MinPower until MinPowerIndex, then iterates backwardly to allocate MaxPower until MaxPowerIndex and finally iterates in between to assign the remaining TPs. We note that strong signal suppression of weaker signals effect can not be totally eliminated in all cases due to the limited, discrete TP levels of LoRaWAN. However, Algorithm 1 minimizes this effect as much as possible.

The run time of our algorithm is linear $O(N)$, where N is the number of nodes per cell since the algorithm iterates over all nodes just once. This is important property because LoRaWAN potentially supports a massive number of nodes per cell. Therefore, our algorithm informally increases running time linearly with the nodes number.

IV. EVALUATION AND DISCUSSION

To evaluate our ideas, we implemented FADR in LoRaSim [4]. LoRaSim is an open-source LoRa simulator that takes into account the capture effect only from the same SF, but otherwise assumes perfectly orthogonal SFs. In order to model collisions more comprehensively, we extended LoRaSim to include the non-perfect orthogonality property of SFs based on the work in [8], which adds a conservative $6dBm$ CIR threshold to all SF pairs. We compared FADR to state-of-art approaches [18] and [4] by conducting multiple experiments that examine almost all factors that affect the algorithm. All experiments were run for a real-time of one day and repeated 10 times with different random seeds.
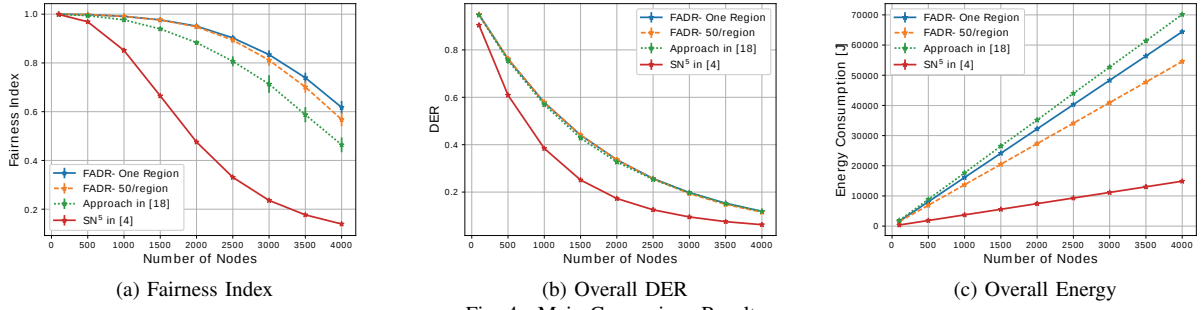
minimum of PowLevels. In case that MaxPower is less than the maximum of PowLevels, the higher values are removed from the list because they will not be used (line 10). This will reduce the energy consumption, thus, extend the nodes' lifetime. Next, the algorithm assigns MinPower to the node with MaxRSSI and MaxPower to the node with MinRSSI, then recalculates MinRSSI and MaxRSSI accordingly (lines 15-16). Subsequently, the algorithm starts allocating the TPs that can be divided into three stages. Firstly, allocating MinPower to high RSSI nodes as long as the new RSSI is not lower than the MinRSSI (lines 18-23). The index of the last node that complies with this approach is saved in MinPowIndex.

Fig. 4. Main Comparison Results

A. State-of-the-art

Authors of [18] present a SF and TP control algorithm to optimize the packet error rate fairness of LoRaWAN. The SFs are allocated by sorting nodes first by their path loss, then by using the optimal distribution ratios Eq. 2, where nodes with the lowest path loss get the lowest SF. The TP control of [18] is based on the observation that nodes with high path loss and $SF8$ are the nodes with the highest packet error rate. Therefore, the algorithm assigns a high enough transmission power to these nodes and allocates $SF7$ and $TP = 2dBm$, i.e. short airtime and low TP, to all nodes that can corrupt these nodes' packets. Then the algorithm iterates again over all nodes to allocate enough TP to all remaining nodes. We argue that this observation depends on the node distribution around the gateway, where these nodes may have lower or higher path loss depending on their locations from the gateway. We show when this assumption can be valid later on.

Authors of [4] show in their SN^5 experiment a way of allocating data rate and TP in which each node chooses its transmission parameter combination locally to minimize first the airtime and secondly the lifetime. A node uses a combination that ensures its packets are received by the gateway and at the same time consumes less energy.

B. Cell lay-out

In this work, we consider a LoRaWAN cell that consists of one gateway located in the cell center and N nodes placed randomly around the gateway. We investigated various cell radii R and various number of nodes that are placed in the cell using different node distributions. Nodes generate data packets of length L using transmission rate λ. A gateway is able to receive a configurable number of concurrent signals $MaxRecv$, based on its number of LoRa transceivers, on the same carrier frequency CF as long as concurrent transmissions use different SFs and are within the safe margin. For a given combination of SF and BW, packets are only decoded by the gateway if their RSSI is higher than the corresponding sensitivity.

We used LoRaSim's propagation model which is based on the log-distance propagation model to calculate the RSSI of a node that transmits with TP. The same propagation model is used in [8] and [15]. Authors of [8] assume that any node, using any transmission parameter combination, is able to reach the gateway regardless of its distance from the gateway.

TABLE II
SIMULATION PARAMETERS

Parameter	Value	Unit
Nodes [N]	100-4000	
Packet Length [L]	80	byte
Transmission Rate [λ]	60	sec
Max Reception [$MaxRecv$]	8	
Cell Radius [R]	100-3200	m
Channel Number	1	
Channel Frequency [CP]	868	MHz
Simulation Time	86400	sec
Random Seeds	10	

To achieve the same assumption, the minimum sensitivity of all SF and BW combinations in LoRaSim was lowered to $-155dBm$, so that all nodes can reach the gateway with all combinations. Simulation parameters are shown in table II.

C. Evaluation Experiments

We conducted various experiments to show the performance evaluation of FADR versus the state-of-the-art. We firstly present the main performance evaluation in Sec. IV-C1. Then, the results are discussed in depth in Sec. IV-C2. Subsequently, the impact of the cell size is shown in Sec. IV-C3 and finally the impact of the node distribution is shown in Sec. IV-C4.

1) Main Comparison: Fig. 4 shows the overall results of this study. Fig. 4a shows the fairness index using Eq. 5, Fig 4b shows the overall DER, and Fig. 4c shows the overall energy consumption. We evaluate FADR with two region configurations. First, in FADR-One Region, the entire cell is considered a single region. The second approach, where nodes are sorted according to their RSSI and then divided into groups of 50 nodes, was proposed in [5]. The data rate *per region* is allocated based on Eq. 4 and TP allocation is based on Algorithm 1.

Overall, both FADR region size approaches surpass the other approaches in terms of fairness without sacrificing the overall DER compared to [18] and with a remarkable improvement compared to SN^5 in [4]. On the other hand, both FADR region size approaches consume overall less energy than the approach in [18] but a higher energy than SN^5 in [4], where all nodes choose to transmit using the lowest TP.

The low fairness and DER performance of SN^5 in [4] is due to the fact that data rate and TP allocation was no studied at the cell level. Rather, nodes choose their transmission

(a) DER vs Distance

(b) DER vs SFs

(c) Transmission Power

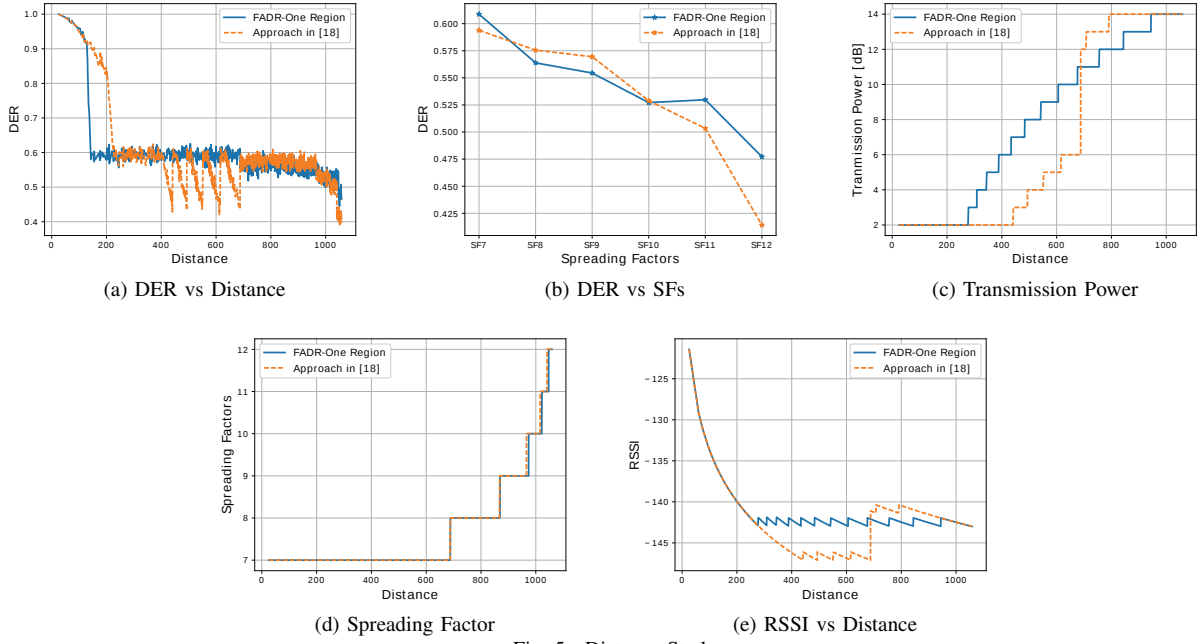(d) Spreading Factor

(e) RSSI vs Distance

Fig. 5. Distance Study

parameter locally, which leads to all nodes choosing the same transmission combination that achieves the lowest airtime and using the lowest TP, which achieves the lowest energy consumption, regardless of the cell status. This leads to a degradation of the cell performance by increasing the number of collisions within the cell and leads to aggressive unfairness for far nodes especially when increasing the number of nodes. In the following, we focus on the impact of the region size and analyze the performance of FADR versus [18] afterwards.

The region size has a notable impact on fairness and overall energy consumption, but almost no impact on the overall DER. Decreasing the region size, on one hand, mixes up all SFs in a small variance of RSSI, on the other hand, SFs are distributed everywhere in the cell, not just in contiguous areas as is the case in single region deployment, which allocates low SFs to high RSSIs and high SFs to low RSSIs. Therefore, small regions serve high SFs better to the detriment of lower SFs, especially $SF7$, by decreasing the imperfect-orthogonality effect of $SF7$ over high SFs. However, small region deployment increases the impact of the capture effect, especially of $SF7$, because nodes with the same SF now have high variance in their RSSIs. As overall nodes with $SF7$ represent the majority of nodes in a cell, small region deployment leads to lower fairness index, as shown in Fig 4a. However, excluding $SF7$ from the analysis and recalculating the fairness index shows that the small region deployment achieves higher fairness than single region deployment.

In terms of energy consumption, the FADR TP control algorithm assigns high TPs to low RSSI and vice versa, which leads to single region deployment consuming higher energy than small region deployments. The reason for this is that the nodes with low RSSI, in single region deployment, are allocated with high SFs, i.e. high airtime, and transmit

using high TPs, but in small region deployments SFs are distributed over the whole cell, thus, airtimes are distributed over TPs as well.

2) Distance Study: Figure 5 shows DER (Fig. 5a), transmission powers (Fig. 5c), SF distribution (Fig. 5d), and RSSIs (Fig. 5e) versus distance in addition to DER per SF (Fig. 5b). These figures provide insights as to why FADR outperforms the approach published in [18]. The results of this study were collected from a cell with 1000 nodes, but we performed the same experiment with a larger number of nodes and got the same behavior.

FADR's advantage over [18] is shown in Fig. 5a in which FADR achieves roughly the same DER for a larger proportion of the network compared to [18] making FADR fairer. Between 400-700m, Reynders' approach [18] experiences high variation in the DER, corresponding to nodes using $SF7$ and low RSSIs. These nodes suffer from an aggressive capture effect by other nodes using $SF7$ and higher RSSIs and at the same time suffer from a capture effect due to the non-orthogonality of SFs from nodes using different SFs and higher RSSIs as shown in Fig. 5e because they do not get enough TP as shown in Fig. 5c.

It seems that the TP control algorithm in [18] provides a TP boost to nodes with $SF8 - 12$ over nodes with $SF7$ and low RSSIs as shown in Fig. 5c. This boost yields an advantage to nodes with high SFs over low RSSI nodes with $SF7$ (these low RSSI nodes suffer from low DER as shown in Fig. 5a) by reducing their non-orthogonality impact on high SFs. However, this boost creates a non-orthogonality impact from $SF8 - 9$ over higher SFs if their RSSIs surpass RSSI of nodes using higher SFs by the safe margin as shown in Fig. 5b. Because fewer nodes use $SF10 - 12$ than use $SF8 - 9$, [18] has slightly higher overall DER, but lower
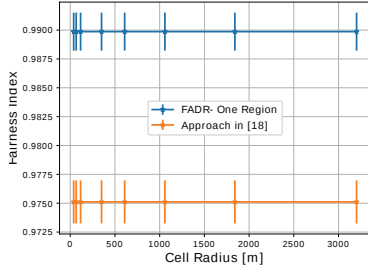
Fig. 6. Cell Size Study

fairness than FADR. This TP boost is the reason for a higher energy consumption compared to FADR.

On the other hand, our FADR TP control algorithm increases the TP gradually and within the safe margin after reaching the minimum limit of using the minimum TP independently of the SF. This ensures that a large proportion of distances around the gateway have a balanced RSSI within the safe margin. With FADR, the nodes close to the gateway have an equal impact over the rest of the cell's nodes. This leads to a slight reduction in the overall DER. However, the DER will be more uniform over distance leading to higher fairness as shown in Fig. 5a and Fig. 5b.

3) Cell Size Study: We investigated the impact of the cell radius, while keeping the number of nodes constant, on the fairness, with results shown in Fig. 6. Increasing the cell radius should provide an increase in the difference of nodes' RSSIs at the gateway. The result shown are collected from a cell with 1000 nodes. However, the behavior is identical to scenarios with other number of nodes. As shown, the cell radius does not have any impact on the fairness of either algorithms, where the difference is always the same. The reason for this is the slow increase in path loss when moving further away. For example, the difference of the RSSIs experienced at $1Km$ cell radius is ca. $62dBm$ and ca. $72dBm$ for $3Km$ cell radius. The $10dBm$ difference between the two cell radii can be handled well within the safe margin of either algorithms.

4) Node Distribution Study: We used the node distribution implemented in LoRaSim in all aforementioned studies, which randomly distributes the nodes around the gateway. Changing the node distribution will affect the performance of either algorithms. in regard of [18], it changes the location of the nodes with $SF8$, which is the reference for this approach. In regard to FADR, it changes the distribution of collisions between nodes. Therefore, to investigate the impact of different node distributions, the cell is divided into three areas (inner, middle and outer), each 0.33 of the cell radius. Then the distribution of the nodes was adjusted to allocate 66.6% of nodes to one area and the rest was uniformly distributed in the other two areas. Therefore, the inner distribution, for example, has 66.6% of nodes in the inner 33% of the cell radius. Fig. 7 shows the DER (Fig. 7a), Fairness (Fig. 7b), and Energy consumption (Fig. 7c) in the different node distributions. The results shown were collected from a cell with 4000 nodes in each distribution.

Overall, the results validate the observations made so far that

the approach in [18] achieves higher DER, but higher energy consumption and lower fairness than FADR with the exception of the inner distribution, where FADR achieves lower fairness. Most of the unfairness in Reynders' approach [18] comes from the impact of the non-orthogonality of low SFs over high SFs in which [18] has higher collisions than FADR. Therefore, FADR from an overall point of view is more suitable for high SFs, i.e. edge nodes, compared to [18]. However, this comes at the expense of DER in the area close to the gateway, where [18] achieves higher DER than FADR.

The inner distribution case is stressful for both approaches because most of the nodes are placed in the high path loss region around the gateway, which affects the remaining 33% of nodes in the rest of the network. The unfairness stems mostly from the impact of non-orthogonality in which [18] has 2.6 times more packets affected by this than FADR. Nevertheless those packets are concentrated in nodes with $SF10-12$ on the outer region of the network. This is because the power boost in nodes with $SF8-9$ is now closer to the gateway, creating a big difference in RSSI larger than the CIR threshold for the nodes in $SF10-12$. Therefore, [18] achieves slightly higher DER in nodes with $SF8-9$, but *zero* DER in nodes with $SF10-12$. Whereas, FADR achieves uniformly distributed DER albeit slightly lower over all those nodes. Due to $SF8-9$ being used by more nodes than $SF10-12$, [18] achieves slightly higher fairness than FADR. However, if the nodes with $SF7$ are not considered, which have much higher DER than all the remaining SFs, FADR achieves 76% fairness, whereas [18] achieves only 64%.

D. Discussion

1) Scalability of Fairness: From the above studies, it should be noted that increasing the number of nodes, i.e. increasing the number of collisions, has a negative impact on the cell fairness. As LoRaWAN has discrete, limited number of TPs $(2-14dBm)$, a cell cannot totally eliminate all collisions using a TP control mechanism. This leads to collisions being not uniformly distributed over distance, but concentrated in certain areas. We see this in the impact of the region of high path loss increase near to the gateway over the rest of the cell. Therefore, increasing the number of collisions magnifies this non-uniformity of collisions, thus, amplifies the unfairness within a cell. Since the transmission rate and the packet length have an impact on the number of collisions as well, these factors affect the fairness as well. While we showed results in this work based on a generated traffic of 80 byte long packets generated once per minute, we found that increasing the transmission rate or packet length with the same number of nodes degrades the fairness.

2) Real World Considerations: The effectiveness of FADR TP control in a real world implementation is affected by the variability of the RSSI, which is not totally stable over time [25]. Therefore, to avoid RSSI instability, FADR is periodically run after collecting a certain number of packets from each node to average over RSSI samples. The number of packets that the algorithm should consider before running is

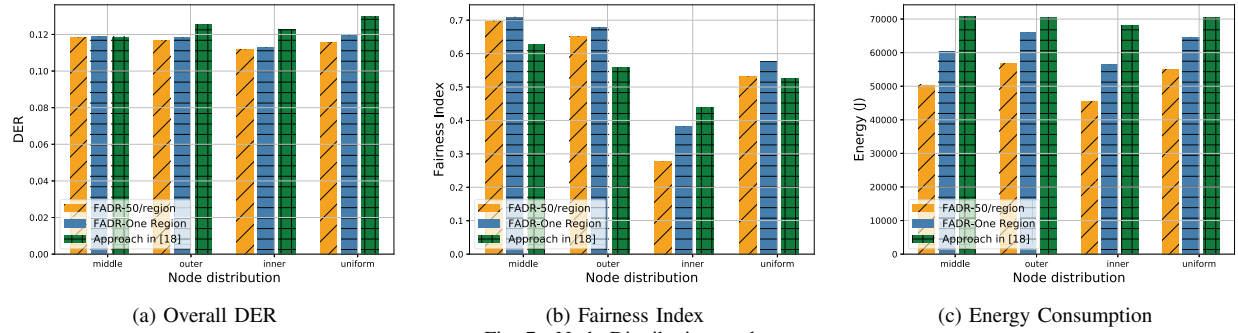(a) Overall DER   (b) Fairness Index   (c) Energy Consumption

Fig. 7. Node Distribution study

under investigation as a future work. Furthermore, it is known that the RSSI values are highly correlated with the propagation model. We used the same log-distance propagation model as in the state-of-art work we compared our approach to. However, we argue the propagation model should not aggressively affect FADR's behavior because FADR does not depend on the RSSI values, but the difference between RSSI values, making FADR more relevant for real world implementations than other approaches that depend on the path-loss estimation. However, as a future work we plan to test FADR's behavior using different propagation models and in real world deployments.

V. CONCLUSION

We proposed FADR to achieve a fair data extraction rate in LoRaWAN cells by deploying the fairest data rate ratios that achieve equal collision probability and by controlling transmission power such that it balances the nodes' received power within a safe margin, thus mitigating the capture effect. FADR achieves an almost uniform data extraction rate for all nodes regardless of their distances from the gateway and maintains the nodes' lifetime by not using excessively high transmission power levels. We implemented and compared FADR to other relevant state-of-art work for various network configurations, which showed FADR's advantages.

ACKNOWLEDGMENT

REFERENCES

[1] U. Raza, P. Kulkarni, and M. Sooriyabandara, "Low power wide area networks: An overview," *IEEE Communications Surveys & Tutorials*, vol. 19, no. 2, pp. 855–873, 2017.

[2] K. Mikhaylov, J. Petäjärvi, and J. Janhunen, "On lorawan scalability: Empirical evaluation of susceptibility to inter-network interference," in *EuCNC*, June 2017, pp. 1–6.

[3] C. Goursaud and J.-M. Gorce, "Dedicated networks for iot: Phy/mac state of the art and challenges," *EAI endorsed transactions on Internet of Things*, 2015.

[4] M. Bor, U. Roedig, T. Voigt, and J. Alonso, "Do lora low-power wide-area networks scale?" in *MSWiM*, 2016.

[5] K. Q. Abdelfadeel, V. Cionca, and D. Pesch, "Poster: A fair adaptive data rate algorithm for lorawan," in *International Conference on Embedded Wireless Systems and Networks*, ser. EWSN '18. ACM, 2018.

[6] S. Corporation, "An1200.22, lora modulation basics," *semtech.com/images/datasheet/an1200.22.pdf*, 2015, online; accessed 10-December-2017.

[7] S. Corporation, "Lora modem design guide," *semtech.com/images/datasheet/LoraDesignGuide$_S$TD.pdf*, 2013, online; accessed 10-December-2017.

[8] D. Croce, M. Gucciardo, I. Tinnirello, D. Garlisi, and S. Mangione, "Impact of spreading factor imperfect orthogonality in lora communications," in *International Tyrrhenian Workshop on Digital Communication*. Springer, 2017, pp. 165–179.

[9] T. Committee, "Lorawan 1.1 specification," 2017, loRa Alliance.

[10] T. Committee, "Lorawan 1.1 regional parameters," 2017, loRa Alliance.

[11] R. Oliveira, L. Guardalben, and S. Sargento, "Long range communications in urban and rural environments," in *ISCC*, July 2017, pp. 810–817.

[12] P. Juha, M. Konstantin, P. Marko, J. Janne, and I. Jari, "Performance of a low-power wide-area network based on lora technology: Doppler robustness, scalability, and coverage," *International Journal of Distributed Sensor Networks*, vol. 13, no. 3, 2017.

[13] D. Bankov, E. Khorov, and A. Lyakhov, "Mathematical model of lorawan channel access," in *WoWMoM*, June 2017, pp. 1–3.

[14] O. Georgiou and U. Raza, "Low power wide area network analysis: Can lora scale?" *IEEE Wireless Communications Letters*, vol. 6, no. 2, pp. 162–165, April 2017.

[15] D. Magrin, M. Centenaro, and L. Vangelista, "Performance evaluation of lora networks in a smart city scenario," in *ICC'17 SAC-7 IoT*, May 2017, pp. 1–7.

[16] M. Bor and U. Roedig, "Lora transmission parameter selection," in *DCOSS*, 2017, pp. 5–7.

[17] F. Cuomo, M. Campo, A. Caponi, G. Bianchi, G. Rossini, and P. Pisani, "Explora: Extending the performance of lora by suitable spreading factor allocations," in *WiMob*, Oct 2017, pp. 1–8.

[18] B. Reynders, W. Meert, and S. Pollin, "Power and spreading factor control in low power wide area networks," in *ICC'17 SAC-7 IoT*, 2017.

[19] R. Yates, "A framework for uplink power control in cellular radio systems," *IEEE Journal on Selected Areas in Communications*, vol. 13, no. 7, pp. 1341–1347, Sep 1995.

[20] A. Subramanian and A. Sayed, "Joint rate and power control algorithms for wireless networks," *IEEE Transactions on Signal Processing*, vol. 53, no. 11, pp. 4204–4214, Nov 2005.

[21] P. Weber, D. Jckle, D. Rahusen, and A. Sikora, "Ipv6 over lorawan," in *IDAACS-SWS*, Sept 2016, pp. 75–79.

[22] K. Q. Abdelfadeel, V. Cionca, and D. Pesch, "Lschc: Layered static context header compression for lpwans," in *Proceedings of the 12th Workshop on Challenged Networks*, ser. CHANTS '17. ACM, 2017, pp. 13–18.

[23] F. Adelantado, X. Vilajosana, P. Tuset-Peiro, B. Martinez, J. Melia-Segui, and T. Watteyne, "Understanding the limits of lorawan," *IEEE Communications Magazine*, vol. 55, no. 9, pp. 34–40, 2017.

[24] R. Jain, D.-M. Chiu, and W. R. Hawe, *A quantitative measure of fairness and discrimination for resource allocation in shared computer system*. Eastern Research Laboratory, Digital Equipment Corporation Hudson, MA, 1984, vol. 38.

[25] M. Aref and A. Sikora, "Free space range measurements with semtech lora technology," in *IDAACS*, Sept 2014, pp. 19–23.